

Selectivity Fields: Comparative Molecular Field Analysis (CoMFA) of the Glycine/NMDA and AMPA Receptors

Igor I. Baskin, Irina G. Tikhonova, Vladimir A. Palyulin, and Nikolai S. Zefirov*

Department of Chemistry, Moscow State University, Moscow 119992, Russia

Received March 27, 2003

An approach for evaluation of binding selectivity was suggested and exemplified using glycine/NMDA and AMPA receptors. For analyzing the pairwise selectivity, we propose to use the difference between biological activities (expressed as $-\log K_i$) of ligands with respect to different receptor subtypes as a dependent variable for building comparative molecular field analysis (CoMFA) models. The resulting fields (which will be referred to as the “selectivity fields”) indicate the ways of increasing selectivity of binding, inhibition, etc. As an example, CoMFA of a set of pyrazolo[1,5-*c*]quinazolines and triazolo[1,5-*c*]quinazolines was used for considering the binding selectivity with respect to glycine/NMDA and AMPA receptors. In addition, the mapping of these fields onto the molecular models of the corresponding receptors makes it possible to reveal the reasons for experimentally observed selectivity as well as to suggest additional ways of increasing selectivity.

Introduction

The problem of selectivity in protein–ligand binding is an increasingly important research area, since its solution would allow discovering high potency drugs with less adverse effects than ligands that bind to several receptors. What is more, biochemical studies need specific “tools”, which are very selective ligands for receptor subtypes.

In particular, we have developed previously the computer models of ionotropic (NMDA,^{1–4} kainate⁵) as well as all metabotropic (mGluR1–mGluR8)⁶ glutamate receptors. However, we faced the following problems: (1) Which structural differences of the receptors determine their pharmacological differences? (2) Which structural differences of ligands could enhance the selectivity to a particular subtype? (3) How can a selective ligand be constructed? To answer these questions one faces the necessity to develop computational approaches aimed at predicting ligand binding selectivity. Below we consider our first attack of the problem.

Modern computational approaches, which can conventionally be divided into the structure-based and ligand-based methods, play an important part in the drug design process. While the structure-based docking algorithms can generate fairly accurate geometries of ligand–receptor complexes, the ligand-based methods afford rapid construction of rather accurate quantitative QSAR models, from which biological affinity of newly designed ligands can be predicted. However, the majority of computational methods are targeted at discovering high-affinity ligands,^{7–9} while the problem of selectivity is usually not sufficiently treated by them.

The comparative molecular field analysis (CoMFA)¹⁰ is a widely used tool for predicting biological activity of ligands. In the framework of this method, the structures of chemical compounds are described by means of

molecular fields expressed by interaction energies of some probe atoms placed at the nodes of a grid around the molecules. The values of biological activity are related to the values of these interaction energies via PLS statistical models, which usually contain a big number of coefficients, several for each node in the grid. The greatest values of these fitting coefficients can be mapped to the appropriate grid nodes to form representation of some fields, which are usually displayed in some color. These field areas show how the biological activity is changed with the change of molecular fields (in essence, molecular structures). The values of biological activity are typically presented in CoMFA analysis in some energy scale, i.e., their values could be the binding energy, logarithm of the binding or inhibition constant, $\log(1/EC_{50})$, $\log(1/IC_{50})$, etc. In this case, the color of a grid node indicates how molecular fields at this node should change (in essence, how the structures of ligands should be changed) to increase affinity to receptor. For example, the standard SYBYL¹¹ settings presume that the presence of a substituent group near a green node, the absence of a bulky group near a yellow node, the presence of a negatively charged atom near a red node, or a positively charged atom near a blue node increases the affinity of ligand to receptor. This enables discovering novel ligands with increased affinity to a given receptor. Nonetheless, increasing affinity to receptor does not automatically mean increasing selectivity of binding with respect to a given receptor subtype in comparison with binding to another member (the *pairwise selectivity*) or to other members (the *group selectivity*) of the same family of receptors.

To address the problem of the pairwise selectivity, we suggest in this paper to use the *difference between biological activities* (expressed, e.g., as $-\log K_i$) of different receptor subtypes as a *dependent variable* for building CoMFA models. The resulting fields (which will be referred to as “the selectivity fields”) would directly indicate the ways of increasing binding selectivity. In

* To whom correspondence should be addressed: tel. +7-095-9393557; fax: +7-095-9390290; e-mail: zefirov@org.chem.msu.su or zefirov@org.chem.msu.ru.

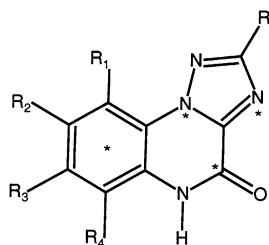


Figure 1. Superimposition criteria of compounds given in Table 1. Fitted elements are labeled with asterisks.

addition, the mapping of these fields onto the molecular models of the corresponding receptors could, in principle, reveal the reasons for experimentally observed selectivity as well as suggest additional ways of increasing selectivity. This approach is illustrated by the example of binding selectivity with respect to glycine/NMDA and AMPA receptors (for models see ref 3).

Results and Discussion

CoMFA Models. CoMFA models were developed using a training set of 52 derivatives of quinazolinone and related compounds (Table 1). Two CoMFA models were built for inhibition constants ($-\log K_i$) with respect to the AMPA and the glycine/NMDA receptors, while the third one was built using *the difference* between $-\log K_i$ for AMPA and glycine/NMDA as a target property. Statistical results of the obtained models are summarized below.

AMPA model: $Q^2 = 0.52$, $R^2 = 0.877$, NOC = 4, $s = 0.258$, St = 56.25, El = 43.75.

Glycine/NMDA model: $Q^2 = 0.528$, $R^2 = 0.890$, NOC = 5, $s = 0.276$, St = 56.15, El = 43.85.

Selectivity model: $Q^2 = 0.608$, $R^2 = 0.894$, NOC = 5, $s = 0.308$, St = 59.9, El = 40.1

(NOC – the optimal number of components as determined by the PLS leave-one-out cross-validation study; s – the standard error of estimate; St and El – the steric and the electrostatic field contributions). As can be seen, the value of Q^2 for the selectivity model is better than other two.

The electrostatic and steric fields for the selectivity model are presented in Figure 2. The electrostatic and steric fields for an ordinary CoMFA analysis are shown in Figure 3. Although they look very similar to the corresponding fields in an ordinary CoMFA study, their meaning is completely different. Selectivity fields depict the change in binding preference occurring upon the change in molecular fields around ligands. For example, for the case depicted in Figure 2, the presence of a substituent near a green region, the absence of a substituent near a yellow region, the increase of a negative charge near a red region or a positive charge near a blue region shift the binding preference toward the AMPA receptor, while the presence of a substituent near a yellow region, the absence of a substituent near a green region, the increase of a negative charge near a blue region, or a positive charge near a red region shift the binding preference in the opposite direction toward the glycine/NMDA receptor. Such fields could, in principle, suggest the way a leading structure should be modified for gaining higher selectivity. Although the value of the standard error of estimate, s , is larger for the selectivity model, one should keep in mind that the

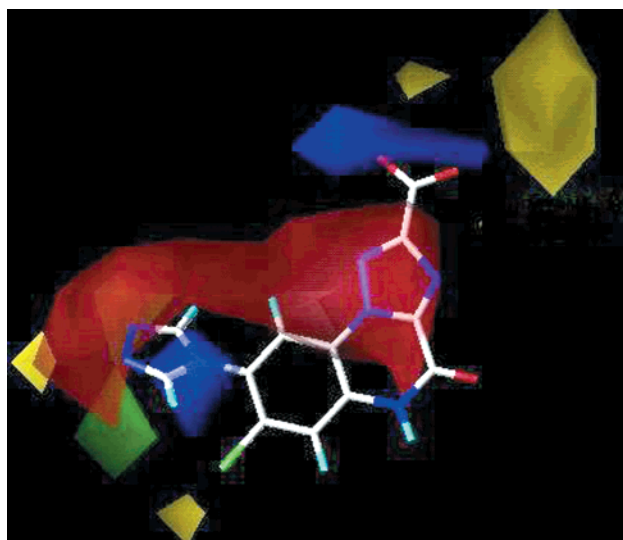
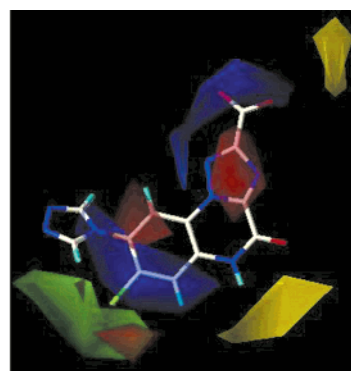
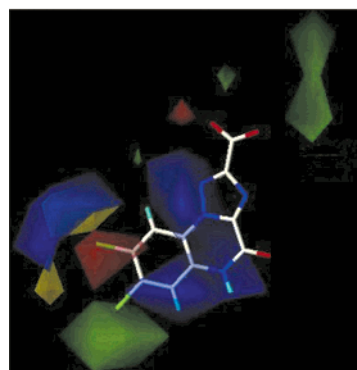


Figure 2. Selectivity fields for AMPA and glycine/NMDA receptors. The presence of a substituent near a green region, the absence of a substituent near a yellow region, and the increase of a negative charge near a red region, or a positive charge near a blue region shift the binding preference toward the AMPA receptor, while the presence of a substituent near a yellow region, the absence of a substituent near a green region, the increase of a negative charge near a blue region, or a positive charge near a red region shift the binding preference in the opposite direction toward the glycine/NMDA receptor.



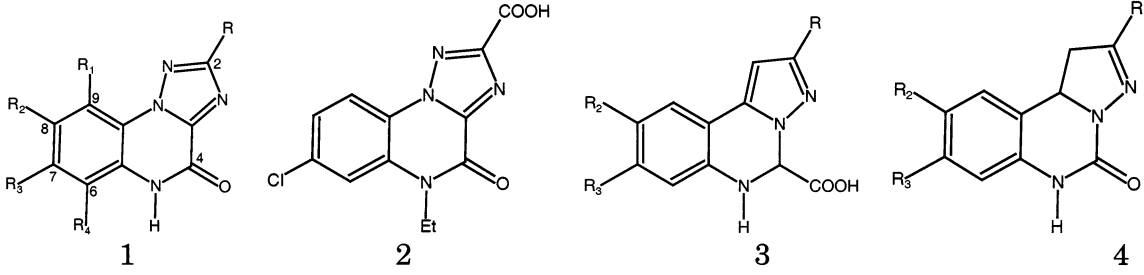
a



b

Figure 3. Steric and electrostatic fields for AMPA (a) and glycine/NMDA (b) receptors. The sterically favored regions are shown in green, and the sterically disfavored regions are shown in yellow. The positive electrostatic contours are shown in blue, and negative electrostatic contours are shown in red.

essence of the standard error of estimate is different in this case. Since the standard deviation of the sum (or difference) of two independent random variables with

Table 1. Structures and Activities of Pyrazolo[1,5-*c*]quinazolines and Triazolo[1,5-*c*]quinazolines Used for the Training Set in CoMFA Analysis


no.	St	R	R ¹	R ²	R ³	R ⁴	K _i (μM) [³ H]AMPA	-log K _i AMPA	K _i (μM) [³ H]glycine	-log K _i glycine	Δ ^a	ref
1	1	COOH	H	imidazol-1-yl	Cl	H	0.14	0.85	33.5	-1.53	2.38	12
2	1	COOEt	H	pyrazol-1-yl	Cl	H	18.4	-1.26	23	-1.36	0.1	12
3	1	COOH	H	pyrazol-1-yl	Cl	H	0.86	0.07	0.86	0.07	0	12
4	1	COOEt	H	2-formyl-pyrazol-1-yl	Cl	H	1.9	-0.28	19	-1.28	1	12
5	1	COOH	H	2-formyl-pyrazol-1-yl	Cl	H	0.53	0.28	28	-1.45	1.73	12
6	1	COOH	H	pyrazol-1-yl	Cl	H	4.3	-0.63	5.3	-0.72	0.09	12
7	1	COOEt	H	NO ₂	Cl	H	47	-1.67	10.24	-1.01	-0.66	12
8	1	COOH	H	NO ₂	Cl	H	1.2	-0.08	2.2	-0.34	0.26	12
9	1	COOH	H	NO ₂	H	H	10.7	-1.03	79.4	-1.9	0.87	12
10	1	COOH	H	NH ₂	Cl	H	4.9	-0.69	3.6	-0.56	-0.13	12
11	1	COOEt	H	H	H	H	28.5	-1.45	16.7	-1.22	-0.23	13
12	1	COOEt	H	H	Cl	H	2.6	-0.41	3.0	-0.48	0.07	13
13	1	COOEt	H	Cl	H	H	72.1	-1.86	88.2	-1.95	0.09	13
14	1	COOEt	Cl	Cl	H	H	4.9	-0.69	4.8	-0.68	-0.01	13
15	1	COOEt	H	Cl	Cl	H	33.9	-1.53	0.71	0.15	-1.68	13
16	1	COOEt	H	H	NH ₂	H	>100	-2	>100	-2	0	13
17	1	COOEt	H	H	Br	H	3.3	-0.52	2.6	-0.41	-0.11	13
18	1	COOH	H	H	H	H	13.6	-1.13	1.1	-0.04	-1.09	13
19	1	COOH	H	H	Cl	H	0.78	0.1	0.17	0.77	-0.67	13
20	1	COOH	H	Cl	H	H	18.4	-1.26	3.5	-0.54	-0.72	13
21	1	COOH	Cl	H	Cl	H	1.53	-0.18	0.14	0.85	-1.03	13
22	1	COOH	H	Cl	Cl	H	1.3	-0.11	0.074	1.13	-1.24	13
23	1	COOH	H	H	CF ₃	H	0.9	0.05	0.57	0.24	-0.19	13
24	1	COOH	H	H	NO ₂	H	0.6	0.22	0.71	0.15	0.07	13
25	1	COOH	H	H	Br	H	4.4	-0.64	0.39	0.4	-1.04	13
26	1	COOH	H	NO ₂	H	H	10.7	-1.03	79.4	-1.9	0.87	13
27	1	COOH	H	NO ₂	Cl	H	1.2	-0.08	2.2	-0.34	0.26	13
28	1	CH ₂ OH	H	H	Cl	H	4.4	-0.64	7.5	-0.88	0.24	13
29	1	CH ₂ CN	H	H	Cl	H	2.0	-0.3	9.7	-0.99	0.69	13
30	1	CH ₂ COOEt	H	H	Cl	H	2.1	-0.32	6.5	-0.81	0.49	13
31	1	CH ₂ COOH	H	H	Cl	H	3.7	-0.57	1.1	-0.04	-0.53	13
32	1	CONHOH	H	H	Cl	H	3.0	-0.48	1.1	-0.04	-0.44	13
33	1	CONHNH ₂	H	H	Cl	H	5.0	-0.7	9.6	-0.98	0.28	13
34	1	CONH ₂	H	H	Cl	H	11.7	-1.07	7.2	-0.86	-0.21	13
35	1	CONH-5-tetrazolyl	H	H	Cl	H	2.4	-0.38	5.1	-0.7	0.32	13
36	1	CONHCH ₂ CH ₂ OH	H	H	Cl	H	7.7	-0.89	27.7	-1.44	0.55	13
37	1	CONHCH ₂ COOCH ₃	H	H	Cl	H	4.1	-0.61	5.4	-0.73	0.12	13
38	1	CONHCH ₂ COOH	H	H	Cl	H	3.2	-0.51	8.8	-0.94	0.43	13
39	2						>100	-2	88.0	-1.94	-0.06	13
40	3	COOEt	H	H	H	H	42	-1.62	33.3	-1.52	-0.1	14
41	3	COOH	H	H	H	H	12.4	-1.09	1.41	-0.15	-0.94	14
42	3	COOEt	H	H	Cl	H	72	-1.86	26.5	-1.42	-0.44	14
43	3	COOH	H	H	Cl	H	2.3	-0.36	0.48	0.32	-0.68	14
44	3	COOH	H	NO ₂	Cl	H	0.74	0.13	1.1	-0.04	0.17	14
45	3	COOH	H	Cl	Cl	H	2.4	-0.38	0.16	0.80	-1.18	14
46	3	COOH	H	imidazol-1-yl	Cl	H	0.14	0.85	8.3	-0.92	1.77	14
47	3	COOEt	H	2-formyl-pyrazol-1-yl	Cl	H	1.4	-0.15	57	-1.76	1.61	14
48	3	COOH	H	2-formyl-pyrazol-1-yl	Cl	H	0.27	0.57	8.2	-0.91	1.48	14
49	4	COOH	H	H	H	H	96	-1.98	2.0	-0.3	-1.68	14
50	4	COOH	H	H	Cl	H	7.2	-0.86	0.24	0.62	-1.48	14
51	4	COOMe	H	Cl	Cl	H	8.5	-0.93	4.0	-0.6	-0.33	14
52	4	COOH	H	Cl	Cl	H	2.65	-0.42	0.19	0.72	-1.14	14

^a (-log K_i (AMPA) + log K_i (glycine)) is presented as Δ.

the same standard deviation σ equals to $\sigma\sqrt{2}$, therefore the value $s = 0.308$ for the selectivity model could result from the value of $0.308/\sqrt{2} = 0.218$ for the standard deviations of individual models. This value is, apparently, smaller than 0.258 for the AMPA model and 0.276 for the glycine/NMDA model. Therefore, the selectivity

model provides here better correlation in comparison with individual models.

As an addition to the internal cross-validation of the models, an external validation was performed on the test set (Table 2) using the selectivity model, the AMPA model, the NMDA model, and the difference of $-\log K_i$

Table 2. Test Set: Prediction of Δ on the Basis of the Selectivity Model and the Difference of Predictions between the AMPA and the NMDA Models^a

no.	St	R	R ¹	R ²	R ³	R ⁴	K_i (μ M) [³ H]AMPA	$-\log K_i$ AMPA	K_i (μ M) [³ H]glycine	$-\log K_i$ glycine	Δ	ref	Δ_{sel}	$-\log K_i$ AMPA Pred	$-\log K_i$ glycine Pred	Δ_{pred}
53	1	COOEt	H	NH ₂	Cl	H	20.4	-1.31	4.8	-0.68	-0.63	12	-0.22	-1.53	-1.34	-0.19
54	1	COOEt	H	H	CF ₃	H	3.6	-0.56	1.8	-0.26	-0.3	13	-0.1	-0.7	-0.77	0.07
55	1	COOH	H	Cl	H	NO ₂	4.0	-0.6	4.5	-0.65	0.05	13	0.16	-0.98	-1.67	0.39
56	3	COOEt	H	NO ₂	Cl	H	8.2	-0.91	10.6	-1.03	0.12	14	0.3	-1.44	-1.94	0.50
57	4	COOMe	H	H	Cl	H	17.3	-1.24	10.6	-1.03	-0.21	14	-0.23	-1.37	-2.10	0.73

^a $(-\log K_i$ (AMPA) + $\log K_i$ (glycine)) is presented as Δ , Δ_{sel} is the predicted value of Δ based on the selectivity model, and Δ_{pred} is the predicted value of Δ based on the separate AMPA and NMDA models.

values predicted by the AMPA and the NMDA models. As can be seen from this table, the selectivity model provides more accurate predictions in comparison with the use of separate AMPA and NMDA models. At present, it is still not quite clear whether the selectivity models always provide more accurate predictions in all cases; further studies are needed to gain deeper insight into this problem.

It is instructive to compare the CoMFA-based selectivity fields with electrostatic and steric fields in individual CoMFA models for binding to each receptor. Figure 3 illustrates the CoMFA electrostatic and steric fields of AMPA and glycine/NMDA receptors, while Figure 2 shows the selectivity fields superimposed on the structure of one of the most active compound in the training set in each case. Comparing the obtained maps, one can observe that the most pronounced areas of selectivity fields are located in the regions, which have opposite colors in the models for AMPA and the glycine/NMDA receptors. In such regions, obviously, the change of the corresponding molecular fields leads to the opposite change in the binding affinity of ligands with respect to each receptor, so the change in the selectivity becomes the greatest. One should also note that colored regions in the selectivity fields occupy less space in comparison with the fields in individual CoMFA models. This means that the selectivity fields present more focused view on the factors affecting the binding selectivity than the simple comparison of the individual CoMFA fields.

Structure-Based Interpretation of Selectivity Fields. It is fairly evident that the difference in the binding affinity of a ligand with respect to different proteins is eventually caused by the difference in their amino acid sequences. Assuming that (a) closely related proteins are usually similarly folded in space and (b) the binding modes of ligands with respect to them are also similar, one can suggest that the nature and relative position of different regions in selectivity fields could be "inferred" from 3D positions of nonconserved amino acids in the binding sites of the proteins.

Indeed, superimposing the aforementioned CoMFA-based selectivity fields with the models of the AMPA and glycine/NMDA binding sites with a docked ligand allows interpreting the position and the color of each of their regions; such a superposition is shown in Figures 4–6. Figure 4 depicts the complex of AMPA-selective ligand **1** (Table 1) with the AMPA receptor, Figure 5 shows the complex of glycine/NMDA-ligand (compound **15** in Table 1) with the glycine/NMDA receptor, whereas Figure 6 contains the superimposed complexes of the ligand **1** with both receptors. The large red area covering

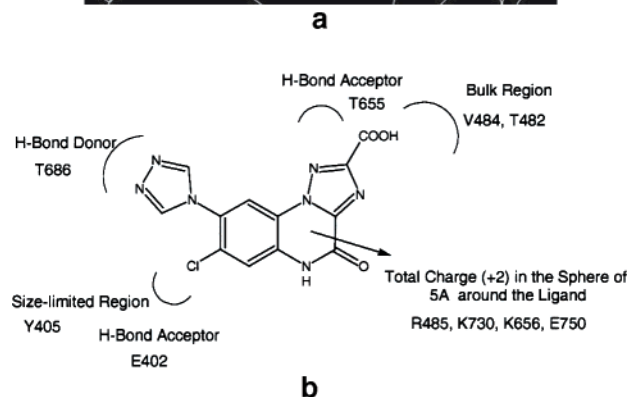
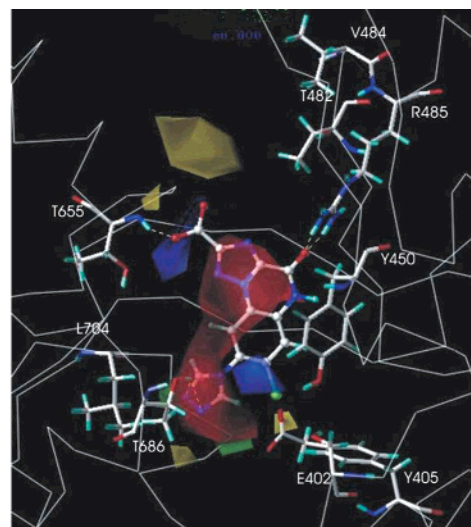


Figure 4. (a) The superimposition of the selectivity fields with the structural model of AMPA receptor and its selective ligand **1** (Table 1). (b) The sketch of the AMPA receptor ligand binding site (shown for ligand **1**).

the central parts of ligands could partially be ascribed to the more positive charge of the binding site in the AMPA receptor in comparison with the glycine/NMDA site.

Actually, the summation of the total charges on amino acids in 5 Å sphere around the ligand gives "+2" for the AMPA receptor (R485, K730, K656, E705) and "-1" (R523, E739, D732) for the glycine/NMDA receptor. This explains the preference of the AMPA receptors to bind negatively charged ligands. The red region close to position 8 of the ligand corresponds to the nonconservative T686 in AMPA receptor and A714 in glycine/NMDA receptor. In this case, the hydroxyl group of T686 serves as a hydrogen-bond donor that binds to acceptor substituents, and therefore compounds with heterocyclic and nitro-substituents have higher affinity to the AMPA receptor as compared to the glycine/NMDA receptor.

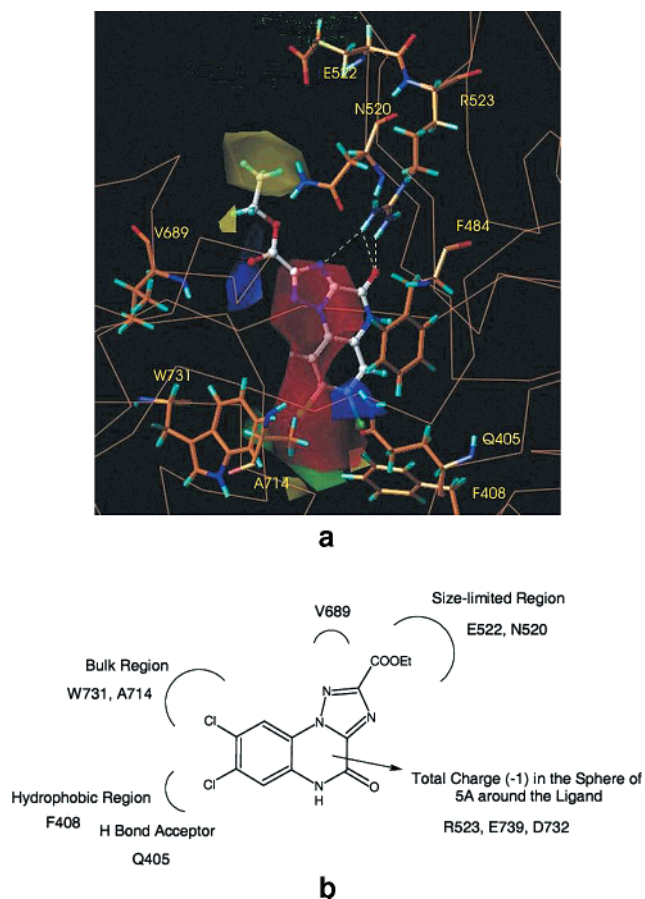


Figure 5. (a) The superimposition of the selectivity fields with the structural model of glycine/NMDA receptor and its selective ligand **15** (Table 1). (b) The sketch of the glycine/NMDA receptor ligand binding site (shown for ligand **15**).

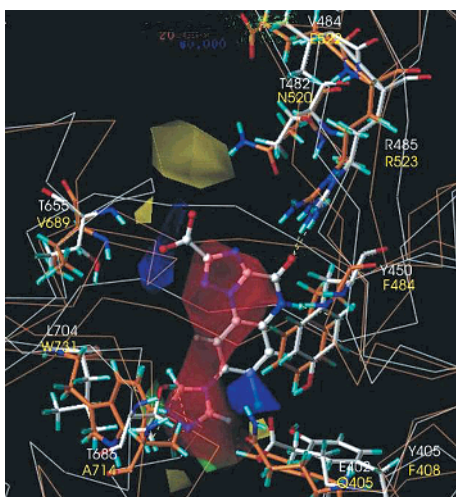


Figure 6. The superimposition of the selectivity fields with the structural model of AMPA and glycine/NMDA receptors. White numbering is used for the AMPA receptor residues and yellow numbering is used for the glycine/NMDA receptor.

The blue area around the carboxyl group of the five-membered ring can be attributed to T655 in the AMPA receptor and V689 in the glycine/NMDA receptor, respectively. In this case, the hydroxyl group of T655 plays a role of a hydrogen-bond acceptor interacting with a hydrogen bond donor substituent. It can also be suggested that the blue area near the 7-position of the ligand corresponds to E402 in AMPA receptor (distance

4.03 Å) and Q405 in glycine/NMDA receptor, respectively (distance 6.0 Å). The large yellow region around the carboxyl group of the five-membered ring can be assumed to correspond to the residue V484 and T482 in AMPA receptor (which causes steric hindrance in this case) and E522 and N520 in glycine/NMDA receptor, respectively. The green area near the 8-position of ligand could be caused either by the preference for substituents in AMPA receptor containing movable L704 or by the steric hindrance in the glycine/NMDA receptor conditioned by W731 in the homologous position. It can also be suggested that the small yellow region near the 7-position is caused by the different nature of Y405 in the AMPA receptor and F408 in the glycine/NMDA receptor.

Consideration of regions in the selectivity fields can be used not only for interpreting known structure–selectivity relationships, but also for designing novel more selective ligands. For example, the presence of the large red area implies that for making ligands more selective to the AMPA receptor electron-withdrawing groups should be introduced in positions 7, 8, and 9, or, alternatively, the carbon atoms in these positions should be substituted for electronegative elements, such as the nitrogen atoms. In particular, according to the CoMFA model, incorporation of a nitrogen atom in positions 9 and 6 of compound **1** (Table 1) increases selectivity (the difference between the affinities to both receptors) to the AMPA receptor from 2.38 to 2.53 and 2.56, respectively. For the case of selectivity with respect to the glycine/NMDA receptor, the substitution of nitrogen atoms to carbon (sp^2 or sp^3) in the five-membered ring significantly increases selectivity to it. On the other hand, the blue region near positions 8 and 7 suggests that placing electronegative halogen as the substituent at these positions should make ligands more selective with respect to the glycine/NMDA receptor. For example, according to the CoMFA model, introduction of the fluorine substituents into position 7 of compound **15** increases selectivity with respect to the glycine/NMDA receptor from -1.68 to -2.57 . In addition, the substitution of positions 7, 8, and 9 of compound **15** by chlorine and fluorine increases selectivity to the glycine/NMDA receptor to 1.959 and 1.83.

Conclusion

The selectivity fields analysis presented in the paper makes it possible to relate chemical structures of ligands with their binding selectivity with respect to different biotargets using the CoMFA technique. It provides a direct and focused view of factors (expressed in terms of CoMFA molecular fields, such as electrostatic or steric ones) affecting the binding selectivity. In principle, such an analysis could suggest modifications that should be introduced to known compounds to design novel more selective ligands.

Since the statistical model for the selectivity field analysis cannot be directly derived from individual CoMFA models, correlations for the selectivity models can be considerably stronger in comparison with them. In such cases, the use of the selectivity field analysis allows making more precise quantitative predictions in comparison with individual CoMFA models.

The additional benefit of using selectivity fields is the ability to perform more accurate receptor mapping as

well as interpretation of molecular fields on the basis of known protein structures, because the number of nonconservative residues in the binding sites of closely related proteins is usually much less than their total number. The knowledge of the nature of residues responsible for each region in the selectivity fields can provide additional information concerning admissible structural changes in ligands.

The selectivity field analysis discussed in this paper is based on using the CoMFA 3D-QSAR analysis, since it provides the most exact binding energy prediction in comparison with alternative approaches, such as the use of scoring functions. However, with the advent of more accurate scoring functions it will be possible to derive selectivity fields based on them. Such fields would be based on the information concerning protein structures rather than on the structures of known ligands, and hence a good representative set of such ligands with measured binding affinity is not needed to develop them.

In this article, only the pairwise selectivity fields have been considered. Evidently, there are many other possibilities, each of which is based on the use of some particular combination of properties as a response variable in the PLS analysis. For example, one can design functions describing the preference of binding to one protein in comparison with binding to some number of others, or the preference of binding to a protein belonging to some subclass in comparison with some other subclass.

Thus, there are many ways of further development of the concept of the selectivity field analysis. The use of this kind of field supplements the CoMFA analysis with additional possibilities.

Methods

Preparation of Ligands for the CoMFA Analysis. The initial structures of 57 compounds (taken from refs 12–14, see Table 1) were prepared using the Sybyl 6.6 molecular modeling software. All molecules were assumed to be protonated under physiological conditions (here we ignore the influence of proteins on the $-\log K_i$ values of ligands bound to them). Their geometry was optimized using the Tripos force field with the Gasteiger-Hückel charges.¹⁵ Low energy conformations were found by systematic¹⁶ and grid conformational¹⁷ searches. For the CoMFA analysis, derivatives of pyrazolo[1,5-*c*]quinazolines and triazolo[1,5-*c*]quinazolines were superimposed using common fitted elements (see Figure 1).

The CoMFA Study. In the present study, the standard Sybyl 6.6 settings for the CoMFA procedure were applied. The CoMFA grid was extended beyond the superimposed molecules by at least 4 Å in all directions of the Cartesian coordinate system. A sp^3 carbon with a charge of +1 served as a probe atom. The CoMFA QSAR equations were derived with the partial least squares (PLS) method. The optimal number of components was selected as providing the highest cross-validation q^2 value. The logarithms of inhibition constant values (K_i) for [³H]AMPA and [³H]glycine/NMDA were used for expressing biological activity (Table 1).^{12–14}

Automated Docking. The crystal structure of AMPASGR (water-soluble AMPA-sensitive glutamate receptor) in complex with antagonist – 6,7-dinitro-2,3-quinoxalinedione (DNQX) was taken from the Brookhaven Protein Data Bank (1FTL).¹⁸ The structure of the glycine/NMDA receptor in the open form was built in our previous work (see ref 3) by homology modeling on the basis of AMPASGR with DNQX. The potential of the protein models was assigned according to the Amber 4.0 force field with Kollman-all-atom charges¹⁹ encoded in Sybyl 6.6.

Lamarckian genetic algorithm (LGA) of Autodock3^{20,21} was used to perform automated molecular docking of several compounds to the AMPA and glycine/NMDA receptors. The number of generations, energy evaluations, and docking runs was set to 570 000, 150 000, and 30, respectively. The final docked complexes of ligand–receptor were selected according to the criteria of interaction energy combined with geometrical matching quality.

Acknowledgment. The authors are grateful to the Russian Foundation for basic research. We also would like to thank Tripos GmbH (Munich, Germany) for scientific and technical assistance.

Note Added after ASAP Posting. This manuscript was released ASAP on 8/9/2003 with errors in the mGluR designations in the third line of the second paragraph of the Introduction. The correct version was posted 8/12/2003.

References

- (1) Tikhonova, I. G.; Baskin, I. I.; Palyulin, V. A.; Zefirov, N. S.; Bachurin, S. O. Structural basis for understanding structure–activity relationships for the glutamate binding site of the NMDA receptor. *J. Med. Chem.* **2002**, *45*, 3836–3843.
- (2) Tikhonova, I. G.; Baskin, I. I.; Palyulin, V. A.; Zefirov, N. S. A spatial model of the glycine site of the NR1 subunit of NMDA-receptor and ligand docking. *Dokl. Biochem. Biophys.* **2002**, *382*, 67–70.
- (3) Tikhonova, I. G.; Baskin, I. I.; Palyulin, V. A.; Zefirov, N. S. CoMFA and Homology-Based Models of the Glycine Binding Site of *N*-Methyl-D-aspartate Receptor. *J. Med. Chem.* **2003**, *46*, 1609–1616.
- (4) Tikhonova, I. G.; Baskin, I. I.; Palyulin, V. A.; Zefirov, N. S. Computer simulation of the three-dimensional structure of the glutamate site of the NR2B subunit of the NMDA receptor. *Dokl. Biochem. Biophys.* **2002**, *382*, 38–41.
- (5) Belenikin, M. S.; Baskin, I. I.; Costantino, G.; Palyulin, V. A.; Pellicciari, R.; Zefirov, N. S. Molecular modeling of the closed forms of the kainate-binding domains of kainate receptors and qualitative analysis of the structure–activity relationships for some agonists. *Dokl. Biochem. Biophys.* **2002**, *386*, 239–244.
- (6) Belenikin, M. S.; Baskin, I. I.; Costantino, G.; Palyulin, V. A.; Pellicciari, R.; Zefirov, N. S. Comparative analysis of the ligand-binding sites of the metabotropic glutamate receptors mGluR1–mGluR8. *Dokl. Biochem. Biophys.* **2002**, *386*, 251–256.
- (7) Kim K. H. Building a bridge between G-protein-coupled receptor modeling, protein crystallography and 3D QSAR studies for ligand design. *Perspect. Drug Discovery Des.* **1998**, *12–14*, 233–255.
- (8) Gane, P. J.; Dean, P. M. Recent advances in structure-based rational drug design. *Curr. Opin. Struct. Biol.* **2000**, *10*, 401–404.
- (9) Makino, S.; Ewing Todd, J. A.; Kuntz, I. D. DREAM++: Flexible docking program for virtual combinatorial libraries. *J. Comput.-Aided Mol. Des.* **1999**, *13*, 513–532.
- (10) Cramer, R. D. III; Patterson, D. E.; Bunce, J. D. Comparative molecular field analysis (CoMFA). 1. Effect of shape on binding of steroids to carrier proteins. *J. Am. Chem. Soc.* **1988**, *110*, 5959–5967.
- (11) SYBYL 6.6; Tripos Inc., 1699 South Hanley Rd., St. Louis, MO 63144 USA.
- (12) Catarzi, D.; Colotta, V.; Varano, F.; Filacchioni, G.; Galli, A.; Costagli, C.; Carla, V. Synthesis, ionotropic glutamate receptor binding affinity, and structure–activity relationships of a new set of 4,5-dihydro-8-heteroaryl-4-oxo-1,2,4-triazolo[1,5-*a*]quinoxaline-2-carboxylates analogues of TQX-173. *J. Med. Chem.* **2001**, *44*, 3157–3165.
- (13) Catarzi, D.; Colotta, V.; Varano, F.; Cecchi, L.; Filacchioni, G.; Galli, A.; Costagli, C. 4,5-Dihydro-1,2,4-triazolo[1,5-*a*]quinoxaline-4-ones: excitatory amino acid antagonists with combined glycine/NMDA and AMPA receptor affinity. *J. Med. Chem.* **1999**, *42*, 2478–2484.
- (14) Varano, F.; Catarzi, D.; Colotta, V.; Filacchioni, G.; Galli, A.; Costagli, C.; Carla, V. Synthesis and biological evaluation of a new set of pyrazolo[1,5-*c*]quinazoline-2-carboxylates as novel excitatory amino acid antagonists. *J. Med. Chem.* **2002**, *45*, 1035–1044.
- (15) Purcel, W. P.; Singer, J. A. *J. Chem. Eng. Data* **1967**, *12*, 235–246. Details of the implementation are given in *SYBYL 6.7 Force Field Manual*; Tripos Inc.: St. Louis, MO, 2000; p 164.
- (16) Details of the systematic search are given in *Sybyl 6.7 Force Field Manual*; Tripos: St. Louis, MO, 2000; p 59.

- (17) Details of the grid search are given in *Sybyl 6.7 Force Field Manual*; Tripos: St. Louis, MO, 2000; p 47.
- (18) Armstrong, N.; Gouaux, E. Mechanisms for activation and antagonism of an AMPA-sensitive glutamate receptor: crystal structures of the GluR2 ligand binding core. *Neuron* **2000**, *28*, 165–181.
- (19) Weiner, S. J.; Kollman, P. A.; Case, D. A.; Singh, C.; Ghio, G.; Alagona, S.; Profeta, P.; Weiner, P. *J. Am. Chem. Soc.* **1984**, *106*, 765–784. Details of the implementation are given in *SYBYL 6.7 Force Field Manual*; Tripos Inc.: St. Louis, MO, 2000; p 100.
- (20) Morris, G. M.; Goodsell, D. S.; Huey, W. E.; Halliday, S.; Belew, R.; Olson, A. J. *Autodock Version 3.0.3*. The Scripps Research Institute, Molecular Graphics Laboratory, Department of Molecular Biology: 1999.
- (21) Morris, G. M.; Goodsell, D. S.; Halliday, S.; Huey, W. E.; Hart, W. E.; Belew, R. K.; Olson, A. J. Automated docking using Lamarckian genetic algorithm and empirical binding free energy function. *J. Comput. Chem.* **1998**, *19*, 1639–1662.

JM030833A